Article

Cell Reports

The Alternative Splicing Regulator Tra2b Is Required for Somitogenesis and Regulates Splicing of an Inhibitory Wnt11b Isoform

Graphical Abstract

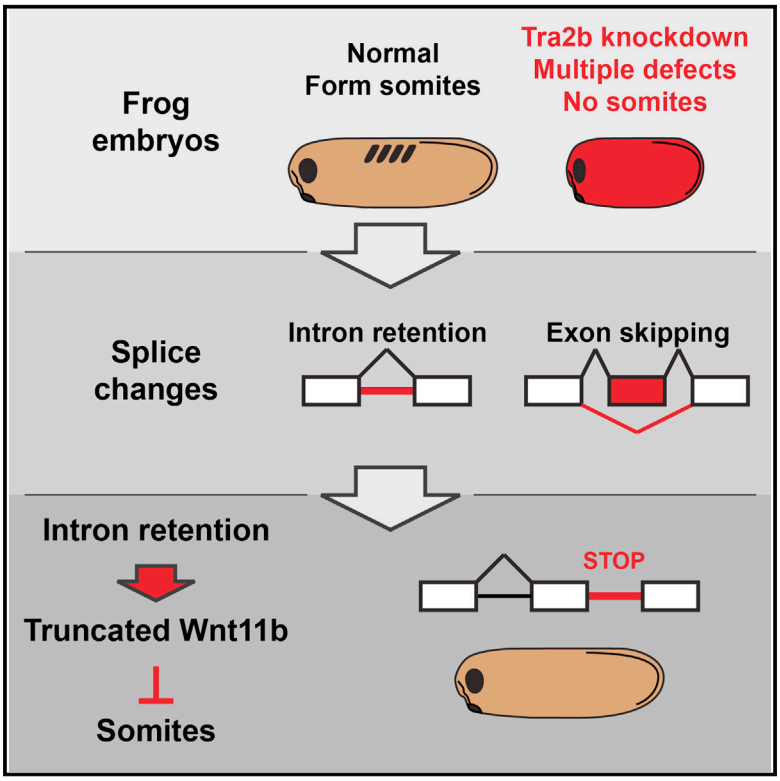

Highlights

- Tra2b knockdown causes multiple developmental defects, including in somitogenesis
- Tra2b knockdown results in intron retention and exon skipping
- Intron retention in wnt11b produces a truncated inhibitory ligand
- The inhibitory Wnt11b ligand inhibits somitogenesis

Authors

Darwin S. Dichmann, Peter Walentek, Richard M. Harland

Correspondence

dichmann@berkeley.edu (D.S.D.), harland@berkeley.edu (R.M.H.)

In Brief

Alternative splicing is pervasive in vertebrates, but the function and regulation of most isoforms are unknown. Here, Dichmann et al. show that the splicing regulator Tra2b is critical for embryogenesis and somite formation. Tra2b regulates an intron retention event in *wnt11b*, which produces a truncated ligand that inhibits somitogenesis.

Dichmann et al., 2015, Cell Reports *10*, 527–536
February 3, 2015
http://dx.doi.org/10.1016/j.celrep.2014.12.046

CellPress

Cell Reports
Article

The Alternative Splicing Regulator Tra2b Is Required for Somitogenesis and Regulates Splicing of an Inhibitory Wnt11b Isoform

Darwin S. Dichmann,[1,*] Peter Walentek,[1] and Richard M. Harland[1,*]
[1]Department of Molecular & Cell Biology, 142 Life Sciences Addition #3200, University of California, Berkeley, Berkeley, CA 94720-3200, USA
*Correspondence: dichmann@berkeley.edu (D.S.D.), harland@berkeley.edu (R.M.H.)
http://dx.doi.org/10.1016/j.celrep.2014.12.046

SUMMARY

Alternative splicing is pervasive in vertebrates, yet little is known about most isoforms or their regulation. *transformer-2b (tra2b)* encodes a splicing regulator whose endogenous function is poorly understood. Tra2b knockdown in *Xenopus* results in embryos with multiple defects, including defective somitogenesis. Using RNA sequencing, we identify 142 splice changes (mostly intron retention and exon skipping), 89% of which are not in current annotations. A previously undescribed isoform of *wnt11b* retains the last intron, resulting in a truncated ligand (Wnt11b-short). We show that this isoform acts as a dominant-negative ligand in cardiac gene induction and pronephric tubule formation. To determine the contribution of Wnt11b-short to the *tra2b* phenotype, we induce retention of intron 4 in *wnt11b*, which recapitulates the failure to form somites but not other *tra2b* morphant defects. This alternative splicing of a Wnt ligand adds intricacy to a complex signaling pathway and highlights intron retention as a regulatory mechanism.

INTRODUCTION

Genome sequencing projects have shown that complex animals and simpler fruit flies and nematodes have a similar number of genes, raising the question of how increased complexity in anatomy and behavior is encoded. Alternative splicing, which creates multiple transcript isoforms from a single gene, is unusual in simple animals but increases with organismal complexity, raising the possibility that alternative splicing serves as a mechanism for expanding protein diversity (Nilsen and Graveley, 2010). Indeed, more than 90% of all human multiexon genes are alternatively spliced (Wang et al., 2008), and many diseases are caused by mutations that perturb either constitutive or alternative splicing (Cooper et al., 2009).

Constitutive pre-mRNA splicing is catalyzed by the spliceosome, a large molecular machine that contains U1–U6 RNAs and several hundred proteins (Will and Lührmann, 2011; Zhou et al., 2002). Alternative uses of splice sites are regulated by auxiliary RNA-binding proteins that bind to the pre-mRNA and either facilitate or repress the use of nearby splice sites (Matlin et al., 2005).

Vertebrate Transformer-2b (Tra2b) is a serine- and arginine-rich (SR)-like protein that contains an RNA recognition motif (RRM) flanked by two SR domains (Segade et al., 1996). The *Drosophila* homolog, Tra2 promotes splicing and regulates sex determination through a cascade of alternative splicing (Black, 2003). Less is known about the biological function of vertebrate Tra2b, although it has been implicated in several human diseases, including cancer (Watermann et al., 2006). Homozygous *tra2b* mutant mice die during embryogenesis, but the cause is unknown (Mende et al., 2010). Interestingly, heterozygous mutant mice are morphologically normal but are obese due to dysfunctional lipid metabolism, indicating that the amount of Tra2b protein must be correctly calibrated (Pihlajamäki et al., 2011). Selective knockout of *tra2b* in the nervous system results in increased apoptosis and disorganized brain structure (Roberts et al., 2014). However, in none of these cases is it known which splicing changes underlie the biological defects.

We isolated *tra2b* in a screen for potent mRNA-encoded bioactivities that affect development (Dichmann et al., 2008). Here, we show that *tra2b* is essential for multiple aspects of normal development in *Xenopus*, including extension of the anterior-posterior axis, somitogenesis, and pronephros formation, all of which are consistent with altered Wnt signaling. Wnt signaling is critical for embryogenesis and tissue homeostasis (MacDonald et al., 2009; Yang, 2012). In *Xenopus*, two wnt11 genes, *wnt11* (also called *wnt11-r*) and *wnt11b* (Garriock et al., 2005), encode functionally identical proteins whose expression patterns differ: *wnt11b* is expressed zygotically in the developing mesoderm and somites, as well as maternally (Ku and Melton, 1993), whereas both genes are expressed in the neural crest and other tissues at later stages (Garriock et al., 2005; Ku and Melton, 1993; Li et al., 2008; Matthews et al., 2008).

Somite segregation employs multiple signaling pathways, in particular those of fibroblast growth factor (FGF), Notch, retinoic acid, and Wnt. Several Wnt ligands, including Wnt3a and other canonical ligands, have been shown to function during somite formation (Dequéant and Pourquié, 2008). Wnt11 has been shown to function after initial somite formation to direct differentiation of the dermatome and myotome

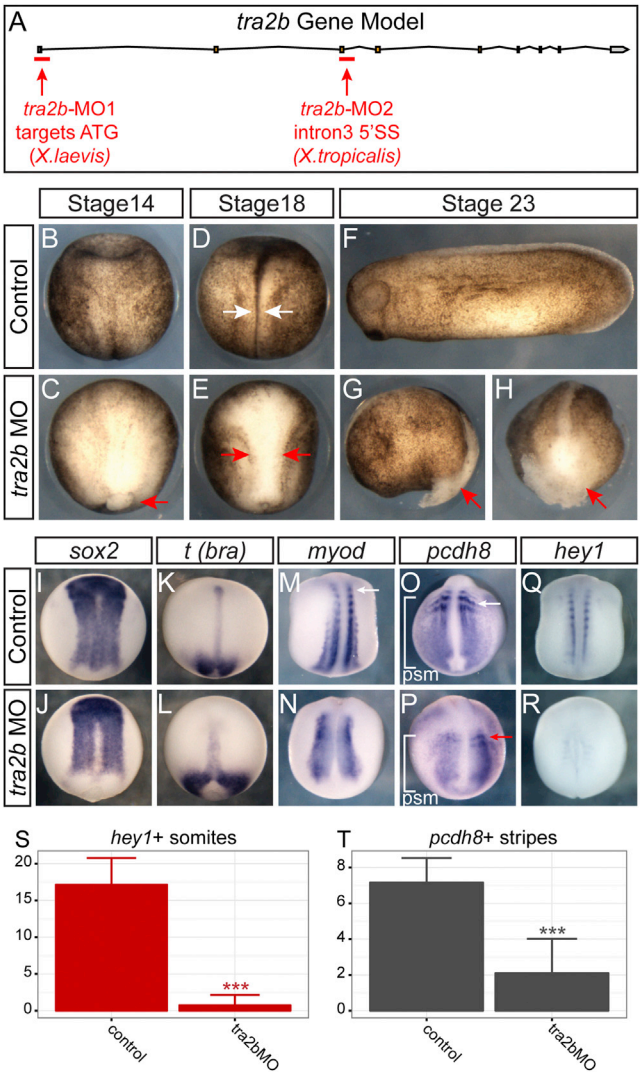

Figure 1. Tra2b Is Required for Somite Formation and Normal Embryogenesis

(A) A translation-blocking MO was used in *X. laevis*, and a splice-blocking MO was used in *X. tropicalis*.

(B and C) Delayed gastrulation in *tra2b* morphants at stage 14; red arrow indicates protruding mesendoderm in morphants (103/110 embryos).

(D and E) Neural tube closure defects at stage 18. White arrows indicate fused neural folds in control embryos; red arrows point to neural folds in the open neural plate of morphants (98/101 embryos).

(F–H) Axis elongation defects and endoderm detachment at stage 23. Red arrows in (G) and (H) indicate endoderm detaching from the embryo through the blastopore (87/99 embryos).

(B–E) Dorsal view with anterior up.

(F and G) Lateral view with anterior to the left.

(H) Posterior view with dorsal up.

(I–R) In situ hybridization (ISH) on control and *tra2b* morphants.

(I–L) Neural plate morphology (*sox2*) and mesoderm specification (*t/bra*) at stage 15.

(M and N) Paraxial mesoderm forms in *tra2b* morphants, but does not segregate into segmented muscle blocks. White arrow in (M) indicates segregated muscle block in control embryo.

(O and P) Presomitic mesoderm (PSM) is present in *tra2b* morphants (white brackets), but presomitic stripe formation is compromised. White arrow in (O) indicates normal stripe pattern, red arrow in (P) points to smaller and fewer stripes in *tra2b* morphants.

(Q and R) Mature somites marked by *hey1* are almost completely absent in *tra2b* morphants.

(S and T) Quantification of *hey1*-positive somites and *pcdh8*-positive stripes in control and *tra2b* morphants. Bars show mean + SD; *** indicates that the difference compared with control is significant at $p < 2.2 \times 10^{-16}$ (t test). Number of embryos used for quantification: 63 (ctrl, *hey1*), 58 (tra2bMO, *hey1*), 68 (ctrl, *pcdh8*), and 59 (tra2bMO, *pcdh8*). Embryos shown are *X. laevis*.

See also Figure S1.

organization (Geetha-Loganathan et al., 2006; Gros et al., 2009; Morosan-Puopolo et al., 2014). In *Xenopus*, somitogenesis is initially highly skewed toward muscle differentiation (Della Gaspera et al., 2012), and Wnt signaling has been implicated in both muscle formation and axial extension (Heisenberg et al., 2000; Hoppler et al., 1996; Tada and Smith, 2000).

Here, we analyze the splicing changes that occur after *tra2b* knockdown, including changes in *wnt11b* that induce expression of a dominant-negative ligand. Our results identify a layer of regulation of the already complex Wnt signaling pathway and highlight the capacity of intron retention (RI) to expand the cell's proteomic repertoire.

RESULTS

tra2b Morphants Have Developmental Defects in All Germ Layers

To determine the function of Tra2b, we designed two morpholino-oligonucleotides (MOs) to knock down Tra2b in either *X. laevis* (*tra2b*-MO1) or *X. tropicalis* (*tra2b*-MO2) (Figure 1A). *X. laevis* embryos injected with *tra2b*-MO1 showed delayed gastrulation and a broadened neural plate at stage 14 (Figures 1B and 1C). At stage 18, *tra2b* morphants had completed gastrulation but failed to close the neural tube (Figures 1D and 1E), and as development proceeded, the morphants failed to extend the anterior-posterior axis, resulting in shortened embryos (Figures 1F and 1G). In addition, the endoderm of *tra2b* morphants dissociated and leaked out of the blastopore prior to hatching (Figures 1G and 1H). This severe and pleiotropic phenotype points to an essential role for Tra2b in multiple processes during embryogenesis, consistent with the broad *tra2b* expression during development (Figure S1). Injection of *tra2b*-MO2 in *X. tropicalis* resulted in an identical phenotype (data not shown). In addition, injection of *tra2b*-MO1 into *X. tropicalis*, or *tra2b*-MO2 into *X. laevis* as mismatch controls (each containing five mismatches to the target sequence in the different species), yielded no phenotype, supporting the specificity of the Tra2b knockdown (data not shown).

To understand the *tra2b* morphant phenotype in detail, we analyzed the expression of developmentally regulated transcripts by in situ hybridization. Expression of the pan-neural marker *sox2* confirmed that neural induction and neural plate morphology were largely normal (Figures 1I and 1J), and expression of the mesodermal marker *t* (*bra*) surrounding the blastopore and notochord during neurulation was normal (Figures 1K and 1L). In contrast, although *myod* was expressed correctly in the

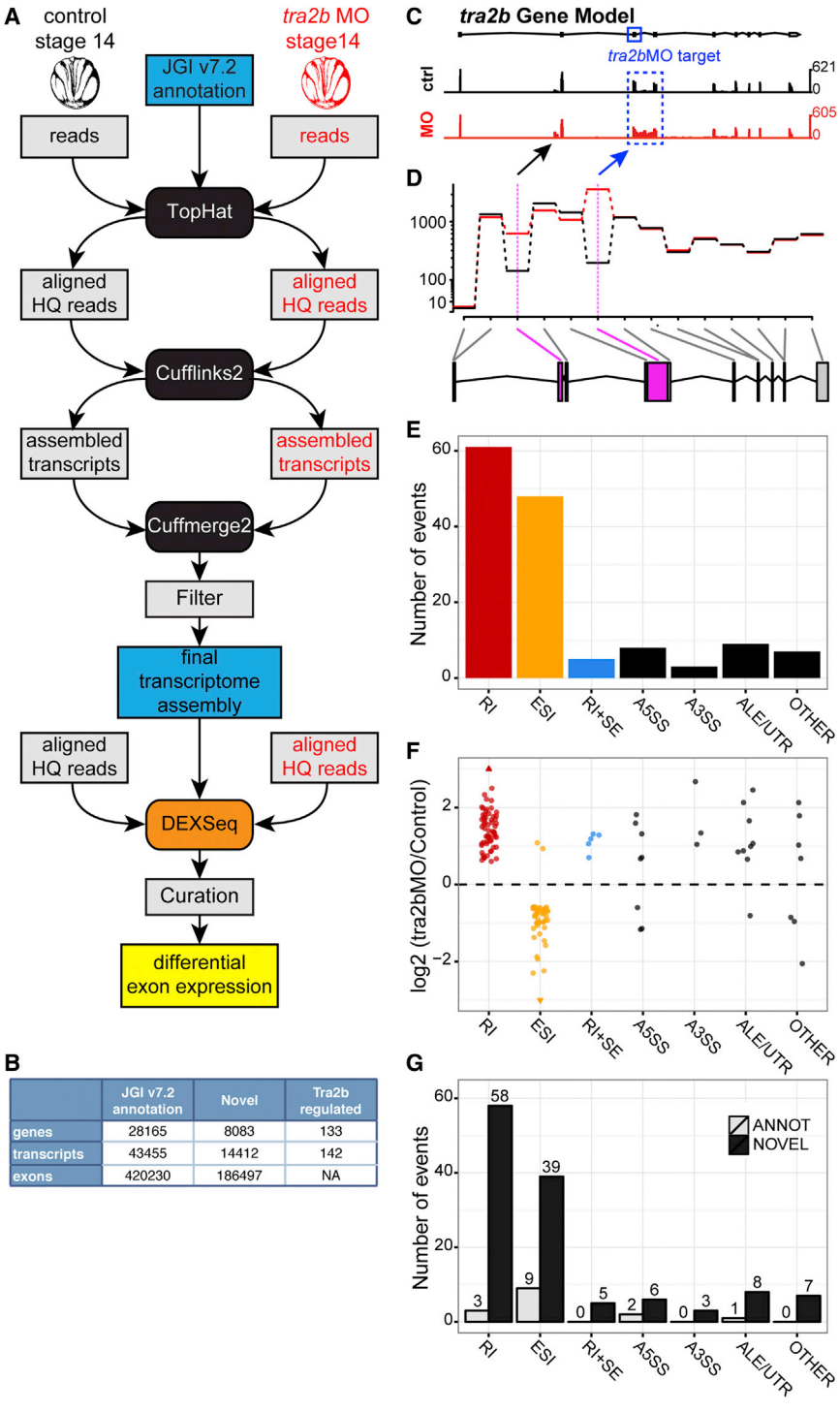

B

	JGI v7.2 annotation	Novel	Tra2b regulated
genes	28165	8083	133
transcripts	43455	14412	142
exons	420230	186497	NA

Figure 2. Analysis of Alternative Splicing in *tra2b* Morphants Shows Intron Retention as the Most Common Splice Change

(A) Outline of the RNA-seq analysis pipeline. Condition-specific transcript assemblies are merged with JGI annotation, resulting in an augmented transcriptome assembly that forms the basis for DEXSeq testing of differential exon expression.

(B) Table showing the number of novel transcripts found in this study and the number of significant splice changes in *tra2b* morphants.

(C) RNA-seq reads from *X. tropicalis* control and morphants in *tra2b* locus show MO-induced intron retention (RI, blue box) and an increase in variable exon 2 (black arrow).

(D) DEXSeq output showing fitted splicing (a proxy for the number of reads aligned) across all exonic regions. Control (black) and morphant (red) exon expression is similar except for the variable exon 2 and MO-induced retained intron, where the graphs diverge. Both events are significant (purple exons indicate adjusted $p < 0.05$).

(E) Alternative splicing changes in morphants grouped by category show RI (red) as the most common event, followed by skipped or included exons (ESI, yellow).

(F) A plot of individual alternative splicing events shows that retained introns are always included in morphants, whereas ESI events in all but two instances are included in normal embryos.

(G) Most of the alternative splicing events detected are novel and are not described in the annotation. See also Figure S2 and Tables S1 and S2.

paraxial mesoderm, it failed to show proper segmentation (Figures 1M and 1N). The failure in axial segmentation was also revealed by *pcdh8*, which is expressed broadly in the presomitic mesoderm (PSM), as well as in stripes where the somites eventually form (Kim et al., 1998), and *hey1*, which marks somites after their formation (Pichon et al., 2002). The PSM, marked by *pcdh8*, was present, but did not show the normal presomitic stripes in *tra2b* morphants (Figures 1O and 1P). Furthermore, *tra2b* morphants failed to form mature somites as judged by *hey1* expression (Figures 1Q–1T). These results argue that defective somitogenesis constitutes an important part of the *tra2b* morphant phenotype.

RNA Sequencing Identifies RI and Exon Skipping as the Primary Splice Changes in *tra2b* Morphants

We used RNA sequencing (RNA-seq) to identify splice changes in *tra2b* morphants. Since *X. laevis* is pseudo-tetraploid, we used the closely related diploid species *X. tropicalis* to simplify our RNA-seq experiments (Hellsten et al., 2010). We employed Cufflinks (Trapnell et al., 2010) to assemble transcripts, using the current JGI transcript annotation (v7.2) as a guide. Importantly, we assembled transcripts separately for the control and MO conditions to increase sensitivity for detecting novel isoforms and used only paired-end sequenced fragments where both reads aligned uniquely (Figure 2A; Tables S1 and S2). We then merged those condition-specific transcript sets into a final transcriptome assembly containing annotated as well as novel

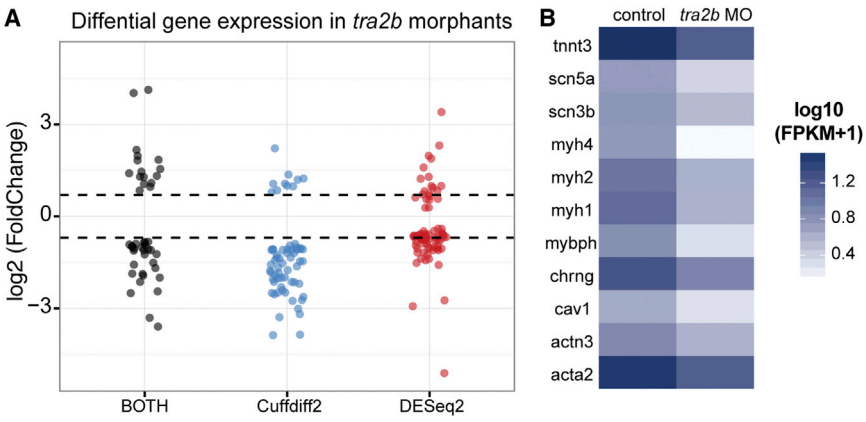

C

GO terms overrepresented in tra2b morphants differentially expressed genes			
Category	**Accession**	**GO Term**	**P-value**
Biological Function	GO:0070252	actin-mediated cell contraction	3.26E-06
	GO:0030049	muscle filament sliding	2.09E-05
	GO:0006936	muscle contraction	5.38E-05
	GO:0006942	regulation of striated muscle contraction	5.72E-05
	GO:0090257	regulation of muscle system process	1.00E-04
Molecular Function	GO:0005516	calmodulin binding	6.19E-03
	GO:0008134	transcription factor binding	7.80E-03
	GO:0008307	structural constituent of muscle	2.53E-05
	GO:0022803	passive transmembrane transporter activity	6.19E-03
	GO:0022838	substrate-specific channel activity	4.38E-03
Cellular Component	GO:0005925	focal adhesion	0.000153
	GO:0015629	actin cytoskeleton	0.00019
	GO:0030055	cell-substrate junction	0.000219
	GO:0005887	integral component of plasma membrane	0.000332
	GO:0030016	myofibril	0.00107

Figure 3. Differential Gene Expression in tra2b Morphants Confirms Reduction of Muscle Transcripts

(A) Comparison of Cuffdiff2 and DESeq2 programs in calling significant changes in gene expression (*X. tropicalis*).

(B) Heatmap showing muscle-related genes that are repressed in *tra2b* morphants.

(C) Table showing the top five enriched GO terms in differentially expressed genes, with muscle-related GO terms indicated in red.

See also Figure S3.

transcripts. Finally, we used DEXSeq (Anders et al., 2012) to detect differential exon expression based on the final annotation. This strategy is highly sensitive for detecting novel isoforms that are predominantly expressed in one set of samples, and thus significantly augments the existing annotation. We also found that the count-based test for differential exon expression used by DEXSeq was more reliable in predicting alternative splice changes than the isoform estimation performed by Cuffdiff2 (a part of the trinity package containing Tophat and Cufflinks). As a final validation, we inspected the read distribution for each predicted splice change on a genome browser and discarded artifactual events (usually a result of incomplete gene models).

Using the Cufflinks/Cuffmerge protocol, we found 14,416 unannotated isoforms in 8,083 already annotated genes, which added increased depth to the genome annotation. The DEXSeq test for differential exon use and subsequent curation identified 142 events that were changed at least 1.5-fold in the number of reads aligned to a region and were significant at adjusted $p < 0.05$ (Figure 2B). The splice changes occurred in 133 different genes. Importantly, the analysis verified the MO-induced RI in *tra2b* transcripts and revealed increased inclusion of a previously unannotated alternative exon 2 in morphants (Figures 2C, 2D, and S2A). This demonstrates our ability to both confirm known splice changes in *tra2b* morphants and detect new ones.

The analysis also revealed a prominent pattern of changes (Figure 2E). The vast majority of changes consisted of whole RI (61 individual events or 43% of total) or whole exon skipping or inclusion (ESI, 48 or 34%), with the rest divided among alternative 5′ or 3′ splice-site usage (A5SS, 6%; A3SS, 2%), combinations of alternative last exons or 3′ UTRs (ALE/UTR, 6%), and complex/other (Other, 5%). Furthermore, we identified five events in which an exon was skipped and the surrounding introns were retained (RI+SE, 4%).

Strikingly, all 61 Tra2b regulated RI events occurred in morphants and none were detected in controls (Figure 2F). Conversely, in the ESI category, all but two events consisted of exons being skipped in *tra2b* morphants (one of the included exons was the variable exon 2 in the *tra2b* transcript itself, as described above). Other categories showed more variation or their smaller sample sizes made it difficult to determine whether they were preferentially used in morphants relative to controls (Figure 2F). Together, these results demonstrate that Tra2b is principally needed to remove a subset of whole introns and to retain a subset of exons.

Among the alternative splicing changes caused by Tra2b knockdown, 126 of the 142 (89%) isoforms that changed in *tra2b* morphants have not been previously described or annotated. Among these, 58 out of 61 RI events and 39 out of 48 ESI events were previously unannotated (Figure 2G).

Muscle-Related Gene Expression Is Reduced in *tra2b* Morphants

In addition to changes in isoform use, we also tested for differential gene expression in *tra2b* morphants to determine whether changes in splicing lead to secondary changes in gene expression. Two software packages, Cuffdiff2 (Trapnell et al., 2012) and DESeq2 (Love et al., 2014), together found 155 differentially expressed genes ($p < 0.05$) with at least a 1.5-fold change in expression (Figure 3A; Table S3). In agreement with the observed defects in mesoderm differentiation, we found several myogenic and muscle-related genes downregulated in *tra2b* morphants (Figure 3B). This was confirmed by a Gene Ontology

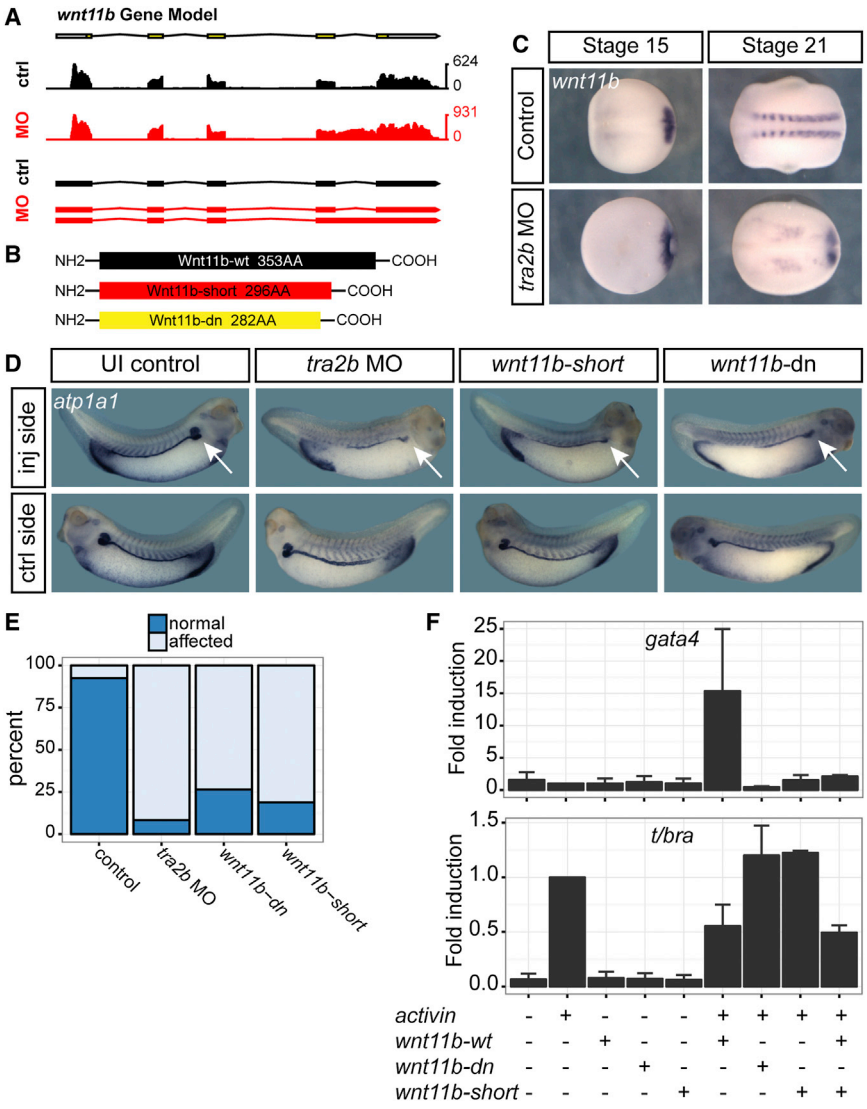

Figure 4. *tra2b* Knockdown Reveals a Novel Inhibitory *wnt11b* Isoform

(A) RNA-seq read profile and Cufflinks assembled transcripts on the *wnt11b* locus show retention of intron 4. The top panel shows the JGI gene model for *wnt11b*, and the middle and bottom panels show read profiles and Cufflinks-assembled transcripts from control and morphants.

(B) Intron 4 retention results in a truncated protein (red, Wnt11b-short) resembling a dominant-negative ligand (yellow) that lacks 57 C-terminal residues compared with normal (black).

(C) *wnt11b* is expressed in the presomitic mesoderm/circumblastoporal region and somites. Embryos are shown in dorsal view with anterior to the left.

(D) *wnt11b-short* mimics *wnt11b-dn* in a pronephric tubule inhibition assay. Embryos were injected unilaterally into the prospective lateral mesoderm and examined by ISH for *atp1a1*, which marks the developing pronephros. Arrows point to the proximal pronephric tubules on the injected side.

(E) Summary of the pronephros tubule inhibition assay. Number of embryos scored: 144 (control), 72 (*tra2b*MO), 87 (*wnt11b-dn*), and 69 (*wnt11b-short*).

(F) qRT-PCR for induced cardiac gene expression (*gata4*) or axial mesoderm (*t/bra*) on animal caps injected with combinations of *activin*, *wnt11b*, *wnt11b-dn*, and *wnt11b-short*, showing that *wnt11b-short* acts similarly to *wnt11b-dn* and counters the effect of *wnt11b*. Bar plots show the mean of three independent experiments + SEM of normalized fold induction compared with *activin*-injected embryos.

(A) shows data from *X. tropicalis* and (C)–(F) show data from *X. laevis*. See also Figure S4.

(GO) term analysis of differentially expressed genes, in which 77 out of 155 frog genes were successfully mapped with human GO terms. GO terms related to muscle function were significantly enriched in all categories (Figure 3C). Using quantitative RT-PCR (qRT-PCR), we confirmed significant inhibition of 10/11 muscle-related transcripts (Figure S3). In summary, our analysis of gene expression changes and the observed somitogenesis defects support a function for Tra2b in mesoderm development.

RI in *wnt11b* Results in Expression of a Dominant-Negative Ligand

Given the prominence of RI in *tra2b* morphants, we sought to determine whether the failure to form somites could be caused by RI in specific transcripts. Indeed, we identified a previously uncharacterized isoform of *wnt11b* that showed a dramatic retention of the last intron (Figure 4A; here named *wnt11b-in4ret*, encoding Wnt11b-short protein). This splice change introduces a premature stop codon immediately within the retained intron, resulting in a truncated protein. Interestingly, this truncated isoform is similar to an engineered dominant-negative Wnt11b (Wnt11b-dn; Figure 4B; Tada and Smith, 2000), raising the possibility that some of the defects observed in *tra2b* morphants are a result of inhibited Wnt signaling. In frogs and zebrafish, *wnt11* orthologs are known to function during early development and gastrulation (Heisenberg et al., 2000; Kofron et al., 2007; Tada and Smith, 2000; Walentek et al., 2013). However, *wnt11b* is also expressed in the PSM and somites, consistent with a function during somitogenesis (Figure 4C). In contrast to *wnt11b*, we found no changes in *wnt11* (*wnt11-r*) transcript level or splicing (data not shown).

To determine whether Wnt11b-short can act as a dominant-negative ligand, we tested its ability to inhibit pronephric tubule formation similarly to Wnt11b-dn (Tételin and Jones, 2010). First, we injected embryos with a low dose of *tra2b* MO targeted to the lateral/intermediate mesoderm, which allowed development to stage 40, when nephrogenesis can be investigated. These morphants had severe defects in forming the proximal pronephric tubules, consistent with the notion that the *tra2b* MO affects nephrogenesis by inducing expression of an inhibitory Wnt11b

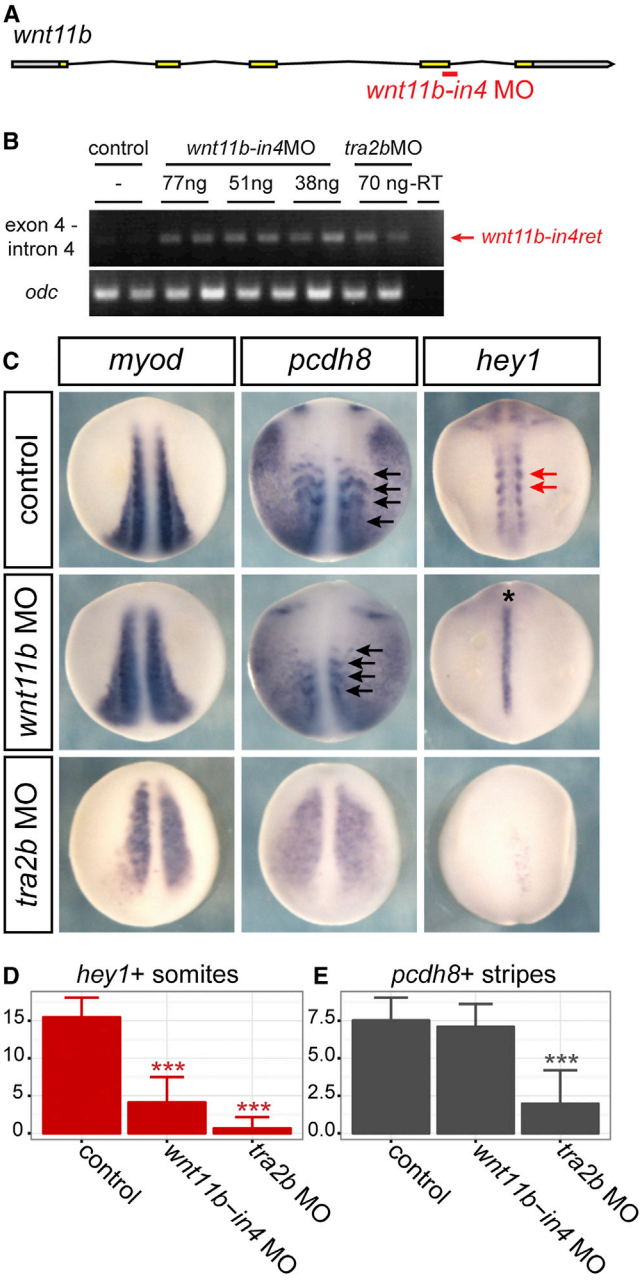

Figure 5. RI in *wnt11b* Is Responsible for Somite Defects in *tra2b* Morphants

(A) Diagram showing *X. laevis wnt11b* gene structure and the *wnt11b-in4* MO (red).

(B) RT-PCR on stage 19 single embryos injected with *wnt11b-in4* MO or *tra2b* MO shows efficient retention of intron 4. The top panel shows RT-PCR with primers in *wnt11b* exon 4 and intron 4, and the bottom panel shows the internal control *odc*.

(C) ISH for mesodermal gene expression in *wnt11b-in4* MO- and *tra2b* MO-injected embryos. Black arrows in *pcdh8*-stained embryos indicate the presence of somitic stripes in control and wnt11b-in4 MO-injected embryos. Red arrows in *hey1*-stained embryos indicate mature somites in control embryos, which are absent in *wnt11b-in4* and *tra2b* morphants. The asterisk (*) in *hey1* samples indicates nonsomitic midline *hey1* expression, which is exposed because of a neural tube closure defect. All pictures show dorsal views with anterior up.

(D and E) Quantification of ISH results, showing the mean and SD of the number of *hey1*+ somites (D) and *pcdh8*+ stripes (E); *** indicates that difference is statistically significant from control at $p < 2.2 \times 10^{-15}$ (t test). Number of embryos used for quantification: 41 (ctrl, *hey1*), 30 (tra2bMO, *hey1*), 43 (wnt11bMO, *hey1*), 42 (ctrl, *pcdh8*), 32 (tra2bMO, *pcdh8*), and 43 (wnt11bMO, *pcdh8*). Data shown are from *X. laevis*.

(Figure 4D). Crucially, injection of a synthetic mRNA (*wnt11b-short*) that encodes Wnt11b-short into the lateral/intermediate mesoderm also repressed proximal tubule formation, at least to the same degree as *wnt11b-dn* (Figure 4E). This in vivo assay suggests that *wnt11b-in4ret* encodes a ligand that is functionally equivalent to Wnt11b-dn.

We also tested the ability of *wnt11b-short* to block cardiac induction in an animal cap assay. Animal caps injected with *activin* mRNA become mesoderm, as marked by expression of *t/bra*, but when stimulated with both *activin* and *wnt11b*, they express the cardiac mesoderm gene *gata4* or *gata6* and reduce *t/bra* expression (Afouda et al., 2008; Pandur et al., 2002; Figures 4F and S4A). Neither *wnt11b-dn* nor *wnt11b-short* coinjected with *activin* induced *gata4* or reduced *t/bra* gene expression, but importantly, coinjection of *wnt11b-short* prevented induction of *gata4* or *gata6* by *activin* and *wnt11b*. As expected, the endodermal marker *sox17* was induced in all *activin*-injected samples, but not in those injected with *wnt11b*, *wnt11b-dn*, or *wnt11b-short* alone (Figure S4A). Together, these animal cap and pronephric tubule experiments strongly argue that *wnt11b-in4ret* encodes a dominant-negative Wnt11b ligand.

While analyzing *wnt11b*, we discovered that the *X. tropicalis* genome contains an unannotated *wnt11b* gene duplication (Figure S4B). This gene (*xetro.H00536*) is adjacent to the annotated *wnt11b* but is transcribed in the opposite direction. Interestingly, *xetro.H00536* also displays retention of the last intron in *tra2b* morphants, suggesting that the target sequences are conserved in the duplicate.

Retention of *wnt11b* Intron 4 Recapitulates the Failure to Form Somites in *tra2b* Morphants

To test whether Wnt11b-short contributes directly to the phenotype of *tra2b* morphants, we specifically induced splicing of *wnt11b-in4ret* using an MO targeting the last exon-intron junction in *wnt11b* in *X. laevis* (Figure 5A). Indeed, RT-PCR on single embryos injected with increasing doses of the *wnt11b-in4*MO showed that the MO was at least as effective at inducing *wnt11b* intron 4 retention as *tra2*MO1 (Figure 5B). Sequencing the amplicons verified that they originated from retention of intron 4.

Next, we analyzed mesoderm and somite development in *wnt11b-in4* morphants and compared them with *tra2b* morphants (Figure 5C). The resulting embryos were short, but did not show some of the other defects of the *tra2b* knockdown, such as endodermal loss. At the molecular level, both control embryos and *wnt11b-in4* morphants had similar axial mesoderm formation at stage 20 as judged by *myod* expression, whereas in *tra2b* morphants, *myod* was severely reduced, as observed earlier. In addition to the near-normal *myod* expression, *wnt11b-in4* morphants showed segmentation stripes of *pcdh8*, although these extended less than in control embryos. In contrast

and as observed earlier, *tra2b* morphants had reduced *pcdh8* expression and little sign of segmentation. Despite the milder effects on early mesoderm development in *wnt11b-in4* morphants, these embryos failed to form mature somites as judged by *hey1* expression. Quantification confirmed that *wnt11b-in4* morphants were similar to control embryos in the number of *pcdh8*-expressing stripes, whereas *tra2b* morphants were reduced to 26% of normal (Figure 5D). Likewise, quantification of *hey1*+ somites in the three classes confirmed that they were reduced to 5% and 27% of normal in *tra2b* and *wnt11b-in4* morphants, respectively (Figure 4E). These results demonstrate that *wnt11b-in4* morphants have a more normal mesoderm development prior to somitogenesis than *tra2b* morphants, yet fail to form *hey1*-positive somites.

Frogs, as well as other vertebrates, possess two transformer-2 genes (*tra2a* and *tra2b*), raising the possibility that Tra2b regulates *wnt11b* splicing through changes in *tra2a*. However, we did not detect any significant changes in splicing or expression levels of *tra2a* in our RNA-seq data (data not shown), indicating that Tra2b regulates splicing of *wnt11b* intron 4 even when *tra2a* expression is normal.

In aggregate, these experiments demonstrate that retention of intron 4 in *wnt11b* is responsible for aspects of defective segmentation in *tra2b* morphants. However, *wnt11b-in4* morphants did not display many of the other defects of *tra2b* morphants, notably, the endoderm dissociation defects prior to hatching. This is unlikely to be a result of low efficacy of the *wnt11b-in4* MO, since intron 4 inclusion was more efficient in *wnt11b-in4* injected embryos than in *tra2b* morphants (Figure 5B). This suggests that other splice changes underlie endoderm dissociation and other defects in *tra2b* morphants.

DISCUSSION

This work represents a systematic analysis of splice changes regulated by Tra2b in a vertebrate. Although mouse *tra2b* mutants have been reported to die during early gestation, the causes and the underlying splice changes are unknown (Mende et al., 2010). However, the early embryonic death of *tra2b* mouse mutants is consistent with the severe developmental defects that we observe in *Xenopus tra2b* morphants, so Tra2b may play a conserved regulatory role.

RI has often been dismissed as a result of erroneous splicing, but recent studies have shown that RI has important regulatory functions during granulocyte and nervous system development (Colak et al., 2013; Wong et al., 2013). In those studies, RI was tied to transcript destruction through nonsense-mediated decay. However, retention of the final intron (as here with *wnt11b*) would not activate such decay, and in such cases truncated protein isoforms may act as inhibitors. Thus, the proper removal of the final *wnt11b* intron mediated by Tra2b provides another example of splicing activities being required to regulate differentiation. Tra2b levels appear to be tightly regulated, as evidenced by the metabolic defects in mouse *tra2b* heterozygotes, and different splicing events may differ widely in their requirement for Tra2b.

We employed a modified version of the standard RNA-seq analysis, and by keeping the control and *tra2b* morphant data sets separate, we were able to increase the sensitivity for isoforms that would otherwise fall below the level of detection. In fact, we significantly augmented the existing annotation with more than 14,000 novel isoforms in more than 8,000 genes, even though Tra2b regulates only a small subset of these isoforms (Figure 2B). This approach, combined with our use of DEXSeq to test for differential expression of exons rather than whole isoforms, enabled us to discover novel splice variants and test them for differential expression with high sensitivity. One surprising observation in this study is that a large majority of the isoforms that we found to be differentially expressed in *tra2b* morphants had not previously been described. Together, these results emphasize the strict requirement for Tra2b in normal development and for splicing of a highly restricted set of isoforms.

The structure of *wnt11b-in4ret* makes it indistinguishable from a partially spliced transcript, but its presence in our RNA-seq data (which were poly-A selected) and inhibition of somitogenesis in *wnt11b-in4* morphants strongly argue that it encodes a functional protein. Detection of endogenous Wnt proteins is notoriously difficult, and we have not successfully detected either Wnt11b isoform. Nonetheless, the inferred presence of an inhibitory Wnt11b ligand adds an additional layer of regulation to the complex Wnt pathway. In addition to serving a function during normal development or later tissue homeostasis, Wnt11b-short dysregulation may also have clinical impact, since regulation of alternative splicing is often changed in cancer (David and Manley, 2010).

Wnt signaling is known to be necessary for somitogenesis. In other vertebrates, Wnt11 has been shown to influence later aspects of somite differentiation and to be involved in epithelial transition of the dermomyotome (Geetha-Loganathan et al., 2006; Morosan-Puopolo et al., 2014). Our experiments involving induced expression of Wnt11b-short in the PSM and somites using the *wnt11b-in4* MO strongly suggest a function for Wnt11b in early phases of somite formation.

Alternative splicing expands proteomic complexity by allowing multiple proteins to be generated from a single locus. More than 90% of all human multiexon genes give rise to more than one isoform (Wang et al., 2008). However, most isoforms have no assigned (or even hypothesized) function, partly because of the lack of a suitable system in which to study alternative splicing in a native organismal context. Here, we exploited the pairing of embryology with global transcriptome analysis to study alternative splicing in *Xenopus*. We specifically connected the splice change in *wnt11b* to defects in somitogenesis, whereas other defects in *tra2b* morphants are unrelated to this splice change. Likely, some of the 141 other splice changes we detected underlie these aspects of the *tra2b* phenotype.

EXPERIMENTAL PROCEDURES

Microinjection of *Xenopus* Embryos

The following MOs (GeneTools) were used in this study: *tra2b*-MO1 (*X. laevis*; translation blocking) 5′-CTCCGCTATCACTCATCTTGTCGTC-3′, *tra2b*-MO2 (*X. tropicalis*; exon 3-intron 3 junction) 5′-AAGTTGCATACCCTGTTTCCAA CAT-3′, *wnt11b*-in4-MO (*X. laevis*; exon 4-intron 4 junction) 5′-GACACAGGA CAGGTAAGCTTATCCT-3′, and standard fluorescein-labeled control MO as tracer. Capped mRNA for microinjection was prepared using the mMessage mMachine Kit (Ambion).

For pronephric tubule formation assays, whole embryos were injected laterally into the two right blastomeres at the four-cell stage (to unilaterally target intermediate mesoderm). The total dose was 3 ng of *wnt11b-dn* or *wnt11b-short*, or 41 ng of *tra2b*-MO1. Fluorescent rhodamine-B dextran lineage tracer (0.5–1.0 mg/ml; Molecular Probes) was used to confirm targeting prior to fixation. Analysis of pronephric tubule formation was performed by comparing injected versus uninjected sides of control and manipulated embryos as previously described (Walentek et al., 2012).

The plasmid used to synthesize *wnt11b-short* was generated by PCR cloning from Wnt11b-pCS2+ plasmid (Tada and Smith, 2000) as the template, using the following PCR forward and reverse primers: 5′-AAAAAAATCGA TATGGCTCCGACCCGTCAC-3′ and 5′-AAAAAAGAATTCTTACCTGTCCTGT GTCCCATATG-3′. The PCR product was cloned into pCS108 using *Cla*I and EcoRI. A pCS2+ plasmid encoding Wnt11b-dn (Tada and Smith, 2000) was used for *wnt11b-dn* synthesis.

This work was done with the approval of the Animal Care and Use Committee of the University of California, Berkeley. The assurance number for the University of California, Berkeley, is A3084-01 and is on file at the NIH Office of Laboratory Animal Welfare.

RNA Isolation and RT-PCR/qPCR

RNA was isolated from single embryos using Trizol (Invitrogen) followed by isopropanol precipitation, one or two phenol-chloroform extractions, and a final ethanol precipitation. For standard RT-PCR, random or oligo-dT primed cDNA was synthesized using SuperScriptII (Invitrogen), and PCR was done using PlatinumTaq (Invitrogen). For qRT-PCR on animal caps, embryos were injected into all blastomeres at the four-cell stage near the animal pole, and animal caps were prepared from 15 (±3) embryos per sample (Sive et al., 2000). The following total doses (4 × 10 nl) of mRNA were used: 1 ng of *Wnt11b* or *Wnt11b-dn* (Tada and Smith, 2000), 1 ng of *Wnt11b-short* (this study), and 0.4 pg of *activin* (Thomsen et al., 1990). Following RNA isolation, cDNA was synthesized using iScript (Bio-Rad), and qPCR was done using SsoAdvanced SYBR Green reagents (Bio-Rad) in technical triplicate on a Bio-Rad CFX96 RT-System C1000 Touch thermal cycler. Expression levels were normalized to the housekeeping genes *ef1-α* and *odc*. Expression was calculated relative to uninjected controls and normalized to the level of *activin* induction in the specific experiment. Triplicate biological replicates were performed. The oligos used are in listed in Table S4. RT-PCR to confirm alternative splice changes in *X. tropicalis* was performed on oligo-dT primed cDNA. Confirmation of muscle gene repression was performed as described above for qRT-PCR.

RNA-Seq Library Construction and Sequencing

Multiplexed Illumina libraries were synthesized using the TruSeq RNA Sample Preparation Kit v2 (Illumina) from *X. tropicalis* stage 14 single embryo RNA isolated using Trizol (Invitrogen). Libraries were prepared from control or *tra2b*-MO2 injected in triplicate. Samples were sequenced at the Vincent J. Coates Genomics Sequencing Laboratory (University of California, Berkeley) on Illumina HiSeq2000 machines. Each library was paired-end sequenced on two independent flow cells, resulting in 2 × 75 and 2 × 60 bp reads after quality trimming of 3′ ends. A summary of sequence yields and alignments is provided in Table S2.

Xenopus Embryos and Microinjection

X. laevis embryos were obtained, cultured, and microinjected according to standard methods (Sive et al., 2000). *X. tropicalis* embryos were collected from natural matings and injected into both blastomeres at the two-cell stage (Khokha et al., 2002). Embryos were staged according to the standard table (Nieuwkoop and Faber, 1994). All experiments were performed at least in triplicate. Statistical testing of the reduction in somites in morphants was performed in R (R Core Team, 2014) using the t.test function.

Bioinformatics

Gene names for the JGI v7.2 annotation were obtained from the previous v7.1 annotation (Dichmann and Harland, 2012). Paired-end RNA-seq reads from either control or *tra2b* morphants that passed basic quality filters were aligned using Tophat2.0.9 (Trapnell et al., 2009) to the *X. tropicalis* genome v7.1, with the JGI v7.2 annotation as a guide, allowing novel splice junctions to be discovered. Only sequenced fragments in which both read mates aligned uniquely were used to assemble transcripts using Cufflinks2.1.1 (Trapnell et al., 2012) for either control or morphants. The resulting two condition-specific transcriptome assemblies were merged with the JGI annotation to produce a merged annotation using Cuffmerge2.1.1. The merged annotation was filtered so that only stranded and named transcripts with class code "j" or "=" were retained, resulting in the final annotation. This final annotation was used as the basis for querying for differential exon expression using DEXSeq v1.8 (Anders et al., 2012). DEXSeq output was filtered for changes of less than 50% and erroneous gene models based on inspection on the genome browsers GBrowse2 (Stein, 2013) and IGV (Robinson et al., 2011). Visualization of read profiles and transcripts for figures were captured from GBrowse2. The number of novel isoforms was determined from the final annotation based on transcripts flagged by Cufflinks with class_code "j" (indicating a novel, spliced transcript sharing at least one junction with an annotated transcript). Human GO terms were mapped to *X. tropicalis* genes and the hypergeometric test for enriched terms was performed using the GOstats Bioconductor package (Falcon and Gentleman, 2007). The aligned reads have been submitted to the NCBI Sequence Read Archive under BioProject ID PRJNA266550. The final annotation of all transcript isoforms can be accessed from http://xenbase.org (James-Zorn et al., 2013) under user-submitted data.

Whole-Mount RNA In Situ Hybridization Probes

The following plasmids used to synthesize antisense probes for in situ hybridization (Sive et al., 2000) have been described previously: *atp1a1* (Tran et al., 2007), *bra(t)* (Smith et al., 1991), *myod* (Hopwood et al., 1989), *pcdh8* (Kim et al., 1998), *sox2* (Grammer et al., 2000), and *wnt11b* (Tada and Smith, 2000). A bluescript plasmid containing a 900 bp fragment of the coding DNA sequence was used to synthesize the *hey1* probe (Pichon et al., 2002).

ACCESSION NUMBERS

The NCBI Sequence Read Archive accession number for the data reported in this paper is PRJNA266550.

SUPPLEMENTAL INFORMATION

Supplemental Information includes four figures and four tables and can be found with this article online at http://dx.doi.org/10.1016/j.celrep.2014.12.046.

AUTHOR CONTRIBUTIONS

D.S.D. designed and performed experiments, conducted the bioinformatics analysis, and prepared the manuscript. P.W. validated Wnt11b-short as a dominant-negative Wnt ligand and contributed to experimental design, interpretation of data, and preparation of the manuscript. R.M.H. supervised the project and contributed to preparation of the manuscript.

ACKNOWLEDGMENTS

We thank Sang-Wook Cha from the Heasman/Wylie lab for the HA-tagged *wnt11b* plasmid, and Masazumi Tada for the *wnt11b*-dn plasmid. We thank Professor Don Rio and members of the Harland lab for fruitful discussions. This work was funded by NIH grants GM42341 and GM086321 to R.M.H. P.W. is supported by a fellowship from the Deutsche Forschungsgemeinschaft (WA 3365/1-1).

Received: August 29, 2014
Revised: November 25, 2014
Accepted: December 18, 2014
Published: January 22, 2015

REFERENCES

Afouda, B.A., Martin, J., Liu, F., Ciau-Uitz, A., Patient, R., and Hoppler, S. (2008). GATA transcription factors integrate Wnt signalling during heart development. Development *135*, 3185–3190.

Anders, S., Reyes, A., and Huber, W. (2012). Detecting differential usage of exons from RNA-seq data. Genome Res. *22*, 2008–2017.

Black, D.L. (2003). Mechanisms of alternative pre-messenger RNA splicing. Annu. Rev. Biochem. *72*, 291–336.

Colak, D., Ji, S.-J., Porse, B.T., and Jaffrey, S.R. (2013). Regulation of axon guidance by compartmentalized nonsense-mediated mRNA decay. Cell *153*, 1252–1265.

Cooper, T.A., Wan, L., and Dreyfuss, G. (2009). RNA and disease. Cell *136*, 777–793.

David, C.J., and Manley, J.L. (2010). Alternative pre-mRNA splicing regulation in cancer: pathways and programs unhinged. Genes Dev. *24*, 2343–2364.

Della Gaspera, B., Armand, A.-S., Sequeira, I., Chesneau, A., Mazabraud, A., Lécolle, S., Charbonnier, F., and Chanoine, C. (2012). Myogenic waves and myogenic programs during Xenopus embryonic myogenesis. Dev. Dyn. *241*, 995–1007.

Dequéant, M.-L., and Pourquié, O. (2008). Segmental patterning of the vertebrate embryonic axis. Nat. Rev. Genet. *9*, 370–382.

Dichmann, D.S., and Harland, R.M. (2012). fus/TLS orchestrates splicing of developmental regulators during gastrulation. Genes Dev. *26*, 1351–1363.

Dichmann, D.S., Fletcher, R.B., and Harland, R.M. (2008). Expression cloning in Xenopus identifies RNA-binding proteins as regulators of embryogenesis and Rbmx as necessary for neural and muscle development. Dev. Dyn. *237*, 1755–1766.

Falcon, S., and Gentleman, R. (2007). Using GOstats to test gene lists for GO term association. Bioinformatics *23*, 257–258.

Garriock, R.J., D'Agostino, S.L., Pilcher, K.C., and Krieg, P.A. (2005). Wnt11-R, a protein closely related to mammalian Wnt11, is required for heart morphogenesis in Xenopus. Dev. Biol. *279*, 179–192.

Geetha-Loganathan, P., Nimmagadda, S., Huang, R., Christ, B., and Scaal, M. (2006). Regulation of ectodermal Wnt6 expression by the neural tube is transduced by dermomyotomal Wnt11: a mechanism of dermomyotomal lip sustainment. Development *133*, 2897–2904.

Grammer, T.C., Liu, K.J., Mariani, F.V., and Harland, R.M. (2000). Use of large-scale expression cloning screens in the Xenopus laevis tadpole to identify gene function. Dev. Biol. *228*, 197–210.

Gros, J., Serralbo, O., and Marcelle, C. (2009). WNT11 acts as a directional cue to organize the elongation of early muscle fibres. Nature *457*, 589–593.

Heisenberg, C.P., Tada, M., Rauch, G.-J., Saúde, L., Concha, M.L., Geisler, R., Stemple, D.L., Smith, J.C., and Wilson, S.W. (2000). Silberblick/Wnt11 mediates convergent extension movements during zebrafish gastrulation. Nature *405*, 76–81.

Hellsten, U., Harland, R.M., Gilchrist, M.J., Hendrix, D., Jurka, J., Kapitonov, V., Ovcharenko, I., Putnam, N.H., Shu, S., Taher, L., et al. (2010). The genome of the Western clawed frog Xenopus tropicalis. Science *328*, 633–636.

Hoppler, S., Brown, J.D., and Moon, R.T. (1996). Expression of a dominant-negative Wnt blocks induction of MyoD in Xenopus embryos. Genes Dev. *10*, 2805–2817.

Hopwood, N.D., Pluck, A., and Gurdon, J.B. (1989). MyoD expression in the forming somites is an early response to mesoderm induction in Xenopus embryos. EMBO J. *8*, 3409–3417.

James-Zorn, C., Ponferrada, V.G., Jarabek, C.J., Burns, K.A., Segerdell, E.J., Lee, J., Snyder, K., Bhattacharyya, B., Karpinka, J.B., Fortriede, J., et al. (2013). Xenbase: expansion and updates of the Xenopus model organism database. Nucleic Acids Res. *41*, D865–D870.

Khokha, M.K., Chung, C., Bustamante, E.L., Gaw, L.W.K., Trott, K.A., Yeh, J., Lim, N., Lin, J.C.Y., Taverner, N., Amaya, E., et al. (2002). Techniques and probes for the study of Xenopus tropicalis development. Dev. Dyn. *225*, 499–510.

Kim, S.H., Yamamoto, A., Bouwmeester, T., Agius, E., and Robertis, E.M. (1998). The role of paraxial protocadherin in selective adhesion and cell movements of the mesoderm during Xenopus gastrulation. Development *125*, 4681–4690.

Kofron, M., Birsoy, B., Houston, D., Tao, Q., Wylie, C., and Heasman, J. (2007). Wnt11/beta-catenin signaling in both oocytes and early embryos acts through LRP6-mediated regulation of axin. Development *134*, 503–513.

Ku, M., and Melton, D.A. (1993). Xwnt-11: a maternally expressed Xenopus wnt gene. Development *119*, 1161–1173.

Li, Y., Rankin, S.A., Sinner, D., Kenny, A.P., Krieg, P.A., and Zorn, A.M. (2008). Sfrp5 coordinates foregut specification and morphogenesis by antagonizing both canonical and noncanonical Wnt11 signaling. Genes Dev. *22*, 3050–3063.

Love, M.I., Huber, W., and Anders, S. (2014). Moderated estimation of fold change and dispersion for RNA-Seq data with DESeq2.

MacDonald, B.T., Tamai, K., and He, X. (2009). Wnt/beta-catenin signaling: components, mechanisms, and diseases. Dev. Cell *17*, 9–26.

Matlin, A.J., Clark, F., and Smith, C.W.J. (2005). Understanding alternative splicing: towards a cellular code. Nat. Rev. Mol. Cell Biol. *6*, 386–398.

Matthews, H.K., Broders-Bondon, F., Thiery, J.P., and Mayor, R. (2008). Wnt11r is required for cranial neural crest migration. Dev. Dyn. *237*, 3404–3409.

Mende, Y., Jakubik, M., Riessland, M., Schoenen, F., Rossbach, K., Kleinridders, A., Köhler, C., Buch, T., and Wirth, B. (2010). Deficiency of the splicing factor Sfrs10 results in early embryonic lethality in mice and has no impact on full-length SMN/Smn splicing. Hum. Mol. Genet. *19*, 2154–2167.

Morosan-Puopolo, G., Balakrishnan-Renuka, A., Yusuf, F., Chen, J., Dai, F., Zoidl, G., Lüdtke, T.H.W., Kispert, A., Theiss, C., Abdelsabour-Khalaf, M., and Brand-Saberi, B. (2014). Wnt11 is required for oriented migration of dermogenic progenitor cells from the dorsomedial lip of the avian dermomyotome. PLoS ONE *9*, e92679.

Nieuwkoop, P.D., and Faber, J. (1994). Normal table of the *Xenopus laevis* (Daudin) (New York: Garland Publishing).

Nilsen, T.W., and Graveley, B.R. (2010). Expansion of the eukaryotic proteome by alternative splicing. Nature *463*, 457–463.

Pandur, P., Läsche, M., Eisenberg, L.M., and Kühl, M. (2002). Wnt-11 activation of a non-canonical Wnt signalling pathway is required for cardiogenesis. Nature *418*, 636–641.

Pichon, B., Taelman, V., Kricha, S., Christophe, D., and Bellefroid, E.J. (2002). XHRT-1, a hairy and Enhancer of split related gene with expression in floor plate and hypochord during early Xenopus embryogenesis. Dev. Genes Evol. *212*, 491–495.

Pihlajamäki, J., Lerin, C., Itkonen, P., Boes, T., Floss, T., Schroeder, J., Dearie, F., Crunkhorn, S., Burak, F., Jimenez-Chillaron, J.C., et al. (2011). Expression of the splicing factor gene SFRS10 is reduced in human obesity and contributes to enhanced lipogenesis. Cell Metab. *14*, 208–218.

R Core Team (2014). R: A Language and Environment for Statistical Computing. R Foundation for Statistical Computing, Vienna, Austria. http://www.r-project.org.

Roberts, J.M., Ennajdaoui, H., Edmondson, C., Wirth, B., Sanford, J.R., and Chen, B. (2014). Splicing factor TRA2B is required for neural progenitor survival. J. Comp. Neurol. *522*, 372–392.

Robinson, J.T., Thorvaldsdóttir, H., Winckler, W., Guttman, M., Lander, E.S., Getz, G., and Mesirov, J.P. (2011). Integrative genomics viewer. Nat. Biotechnol. *29*, 24–26.

Segade, F., Hurlé, B., Claudio, E., Ramos, S., and Lazo, P.S. (1996). Molecular cloning of a mouse homologue for the Drosophila splicing regulator Tra2. FEBS Lett. *387*, 152–156.

Sive, H.L., Grainger, R.M., and Harland, R.M. (2000). Early Development of *Xenopus laevis*: A Laboratory Manual (Cold Spring Harbor, New York: Cold Spring Harbor Laboratory Press).

Smith, J.C., Price, B.M., Green, J.B., Weigel, D., and Herrmann, B.G. (1991). Expression of a Xenopus homolog of Brachyury (T) is an immediate-early response to mesoderm induction. Cell *67*, 79–87.

Stein, L.D. (2013). Using GBrowse 2.0 to visualize and share next-generation sequence data. Brief. Bioinform. *14*, 162–171.

Tada, M., and Smith, J.C. (2000). Xwnt11 is a target of Xenopus Brachyury: regulation of gastrulation movements via Dishevelled, but not through the canonical Wnt pathway. Development *127*, 2227–2238.

Tételin, S., and Jones, E.A. (2010). Xenopus Wnt11b is identified as a potential pronephric inducer. Dev. Dyn. *239*, 148–159.

Thomsen, G., Woolf, T., Whitman, M., Sokol, S., Vaughan, J., Vale, W., and Melton, D.A. (1990). Activins are expressed early in Xenopus embryogenesis and can induce axial mesoderm and anterior structures. Cell *63*, 485–493.

Tran, U., Pickney, L.M., Ozpolat, B.D., and Wessely, O. (2007). Xenopus Bicaudal-C is required for the differentiation of the amphibian pronephros. Dev. Biol. *307*, 152–164.

Trapnell, C., Pachter, L., and Salzberg, S.L. (2009). TopHat: discovering splice junctions with RNA-Seq. Bioinformatics *25*, 1105–1111.

Trapnell, C., Williams, B.A., Pertea, G., Mortazavi, A., Kwan, G., van Baren, M.J., Salzberg, S.L., Wold, B.J., and Pachter, L. (2010). Transcript assembly and quantification by RNA-seq reveals unannotated transcripts and isoform switching during cell differentiation. Nat. Biotechnol. *28*, 511–515.

Trapnell, C., Roberts, A., Goff, L., Pertea, G., Kim, D., Kelley, D.R., Pimentel, H., Salzberg, S.L., Rinn, J.L., and Pachter, L. (2012). Differential gene and transcript expression analysis of RNA-seq experiments with TopHat and Cufflinks. Nat. Protoc. *7*, 562–578.

Walentek, P., Beyer, T., Thumberger, T., Schweickert, A., and Blum, M. (2012). ATP4a is required for Wnt-dependent Foxj1 expression and leftward flow in Xenopus left-right development. Cell Rep. *1*, 516–527.

Walentek, P., Schneider, I., Schweickert, A., and Blum, M. (2013). Wnt11b is involved in cilia-mediated symmetry breakage during Xenopus left-right development. PLoS ONE *8*, e73646.

Wang, E.T., Sandberg, R., Luo, S., Khrebtukova, I., Zhang, L., Mayr, C., Kingsmore, S.F., Schroth, G.P., and Burge, C.B. (2008). Alternative isoform regulation in human tissue transcriptomes. Nature *456*, 470–476.

Watermann, D.O., Tang, Y., Zur Hausen, A., Jäger, M., Stamm, S., and Stickeler, E. (2006). Splicing factor Tra2-beta1 is specifically induced in breast cancer and regulates alternative splicing of the CD44 gene. Cancer Res. *66*, 4774–4780.

Will, C.L., and Lührmann, R. (2011). Spliceosome structure and function. Cold Spring Harb. Perspect. Biol. *3*, pii: a003707.

Wong, J.J.L., Ritchie, W., Ebner, O.A., Selbach, M., Wong, J.W.H., Huang, Y., Gao, D., Pinello, N., Gonzalez, M., Baidya, K., et al. (2013). Orchestrated intron retention regulates normal granulocyte differentiation. Cell *154*, 583–595.

Yang, Y. (2012). Wnt signaling in development and disease. Cell Biosci. *2*, 14.

Zhou, Z., Licklider, L.J., Gygi, S.P., and Reed, R. (2002). Comprehensive proteomic analysis of the human spliceosome. Nature *419*, 182–185.